ELECTRONIC STRUCTURE STUDIES OF NANOCRYSTALLINE DIAMOND GRAIN BOUNDARIES

Peter Zapol,[‡] Michael Sternberg,[§] Thomas Frauenheim,[§]
Dieter M. Gruen,[‡] and Larry A. Curtiss[‡]

[‡]Materials Science and Chemistry Divisions,
Argonne National Laboratory, Argonne, IL 60439

[§]Universität-GH, Paderborn, Fachbereich Physik,
Theoretiche Physik, D-33098 Paderborn, Germany

November, 1999

Submitted to the Proceedings of the Sixth International Symposium on Diamond Materials,

196th Meeting of the Electrochemical Society Meeting

Honolulu, Hawaii October 17-22, 1999

DISCLAIMER

DISCLAIMER

Portions of this document may be illegible in electronic image products. Images are produced from the best available original document.

ELECTRONIC STRUCTURE STUDIES OF NANOCRYSTALLINE DIAMOND GRAIN BOUNDARIES

Peter Zapol,[‡] Michael Sternberg,[§] Thomas Frauenheim,[§]
Dieter M. Gruen,[‡] and Larry A. Curtiss[‡]

[‡]Materials Science and Chemistry Divisions
Argonne National Laboratory, Argonne, IL 60439

[§]Universität-GH, Paderborn, Fachbereich Physik,
Theoretiche Physik, D-33098 Paderborn, Germany

ABSTRACT

Diamond growth from hydrogen-poor plasmas results in diamond structures that are profoundly different from conventionally CVD-grown diamond. High concentration of carbon dimers in the microwave plasma results in a high rate of heterogenous renucleation leading to formation of nanocrystalline diamond with a typical grain size of 3-10 nm. Therefore, up to 10% of carbon atoms are located in the grain boundaries. In this paper we report on density-functional based tight-binding molecular dynamics calculations of the structure of a $\Sigma 13$ twist (100) grain boundary in diamond. Beginning with a coincidence site lattice model, simulated annealing of the initial structure was performed at 1500 K followed by relaxation toward lower temperatures. About one-half of the carbons in the grain boundary are found to be three-coordinated. Coordination numbers, bond length and bond angle distributions are analyzed and compared to those obtained in previous studies.

INTRODUCTION

In contrast to diamond films grown by the traditional method involving CH_4/H_2 mixtures, where micron-size crystallites typically constitute the microstructure of the films, diamond grown from argon plasmas containing carbon is characterized by a microstructure consisting of crystallites with an average size of 3-10 nm.[1] This nanocrystalline diamond can be grown to thicknesses of at least 30 μm from argon/fullerene or argon/methane microwave plasmas. A drastic change in electrical conductivity is observed with reduction in crystallite size, with the material going from an insulator to an electrical conductor. This phenomenon is largely due to the fact that grain boundary carbon in diamond is π-bonded.[2] The grain boundaries are therefore conducting, and because their numbers vastly increase with decreasing crystallite size, the entire film becomes electrically conducting.

In earlier papers[3,4] we proposed a mechanism for the growth of nanocrystalline diamond films that featured C_2 as the growth species. Density functional calculations made for growth on the (110) surface showed that the individual steps in this growth mechanism are energetically very favorable and have small activation barriers. We have

also presented results[5] of the energetics of C_2 insertion into clusters that model the unhydrided and monohydrided (100) surfaces, respectively. These results suggested that the mechanism of diamond growth from dicarbon may be dependent on the degree of hydrogenation of the reconstructed (100) surface. The disparate nucleation rates of diamond crystallites grown in hydrogen-rich vs. hydrogen-poor microwave plasmas may be accounted for qualitatively by these results.

The grain boundaries in nanocrystalline diamond have been the subject of several studies. The structure of twist grain boundaries in diamond was studied by Keblinski *et al*[2] using Tersoff interatomic potentials. They found that (100) grain boundaries are more stable against decohesion than (110) and (111) grain boundaries. Up to 80% of the $\Sigma 29$ grain boundary carbon atoms were found to be three-coordinated. A tight-binding molecular dynamics study of the $\Sigma 29$ grain boundary by Cleri *et al*.[6] indicated that about 40% of the grain boundary atoms are three-coordinated and that the electronic band structure has a broad spectrum of gap states between which a hopping conduction is possible. We recently published results[5] of a periodic density functional calculation of a stacking fault that is a model for the diamond grain boundary with sp^2 bonding across the interface. The electronic structure of diamond with defects is characterized by the presence of π-states in the forbidden gap that are localized on the interfacial atoms. These states produce several broad peaks in the gap.

In this paper we report on new density-functional based tight-binding molecular dynamics calculations of the structure of a $\Sigma 13$ twist (100) grain boundary in diamond. Beginning with a coincidence site lattice model, simulated annealing of the initial structure was performed at 1500 K followed by relaxation toward lower temperatures. Coordination numbers, bond length and bond angle distributions, and electronic structure of the grain boundaries are reported and compared to those obtained in previous studies.

THEORETICAL METHODS

The molecular dynamics calculations were performed using a density functional based tight binding (DFTB) method with self-consistent charges using the approach of Frauenheim, Seifert, *et al*.[7,8] This DFTB method uses a linear combination of atomic orbitals (LCAO) formalism and a local density approach. In this scheme the Kohn-Sham orbitals of the many-atom problem are expressed in terms of an explicit minimal basis set of atom-centered localized valence electron orbitals. The general eigenvalue problem for the many-atom configuration is solved to determine the single particle energies and eigenstates of the system, neglecting contributions of the three-center and crystal-field integrals to the matrix elements. The total energy of a system is written as a sum over a "band structure energy" and a short-range repulsive two-particle interaction term. The latter term is derived from a universal pair-potential resulting from a fitting of potential energy curves from self-consistent field calculations in the local density approximation. These parameters have been determined for carbon previously.[7] Interatomic forces for molecular dynamics can be calculated from analytical expressions for the gradients of the total energy at the atomic positions. The self-consistent charge scheme is based on the second order term in an expansion of energy over electron density fluctuations. This term is expressed through Mulliken charges and calculated self-consistently at each molecular dynamics step.

RESULTS AND DISCUSSION

The DFTB molecular dynamics calculations were done on the $\Sigma 13$ twist (100) grain boundaries in diamond. A unit cell for a periodic model of the grain boundary was initially constructed from the coincidence site lattice model using two grain boundaries per unit cell. A relative rotation of two halves of the crystal by 67.4° around the z-axis gives a planar cell with 13 atoms per (001) plane. Each repeating cell has a thickness of 16 layers and thus contains 208 carbon atoms. Molecular dynamics simulation of the initial structure was performed at 1500 K (approximately corresponding to experimental growth temperatures) for 0.5 ps. Subsequently, simulated annealing was performed at gradually lower temperatures. The total energy curve as a function of time is shown in Fig.1. The resulting structure was further optimized at 0 K using conjugate gradient
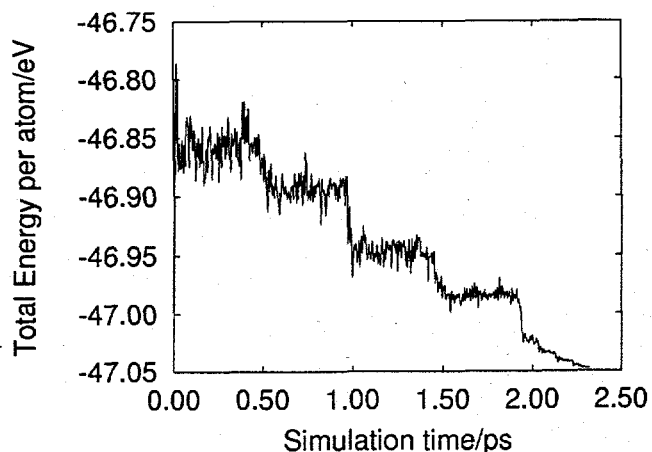

Figure 1. Total energy of molecular dynamics calculation as a function of simulation time.

relaxation and the self-consistent charge scheme until a local minimum was found. This final minimum-energy structure is shown in Fig. 2.
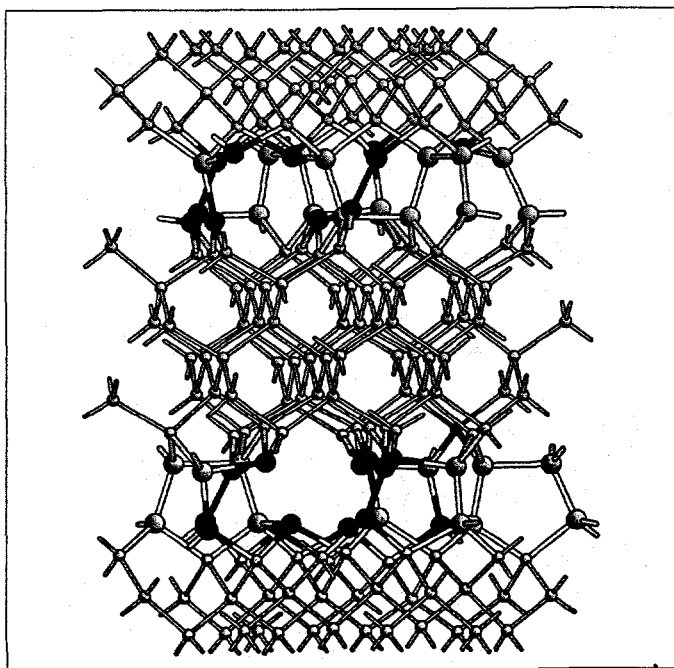

Figure 2. Side view of the periodic cell for an optimized $\Sigma 13$ grain boundary. Two grain boundaries are shown. Black atoms are three-coordinated and gray atoms are four-coordinated. Atoms in the first layers of the interfaces are shown as larger spheres. Bonds extending across the cell boundary are shown as half bonds.

Structural disorder is confined to the two grain boundary planes and the rest of the diamond crystal remains perfectly ordered. Threefold-coordinated atoms constitute 46% of the two grain boundary planes, similar to the tight-binding molecular dynamics results reported by Cleri et al.[6] About half of the three-coordinated atoms have an sp^2 configuration, i.e. have bond angles close to 120° with their neighbors, and the other half have a tetrahedral arrangement of their three bonds, leading to a geometry configuration that is typical for a carbon atom with a dangling bond.

Across the interface, most of the bonds are sp^3-sp^3 single bonds and sp^2-sp^3 partial double bonds. A small number of double bonds are formed between sp^2-like atoms. The structures of the interfacial planes are shown in Fig. 3. It is evident that in addition to bonds formed across the interface, there are many bonds between interface atoms belonging to the same (001) plane. These bonds are related to surface dimers formed on a
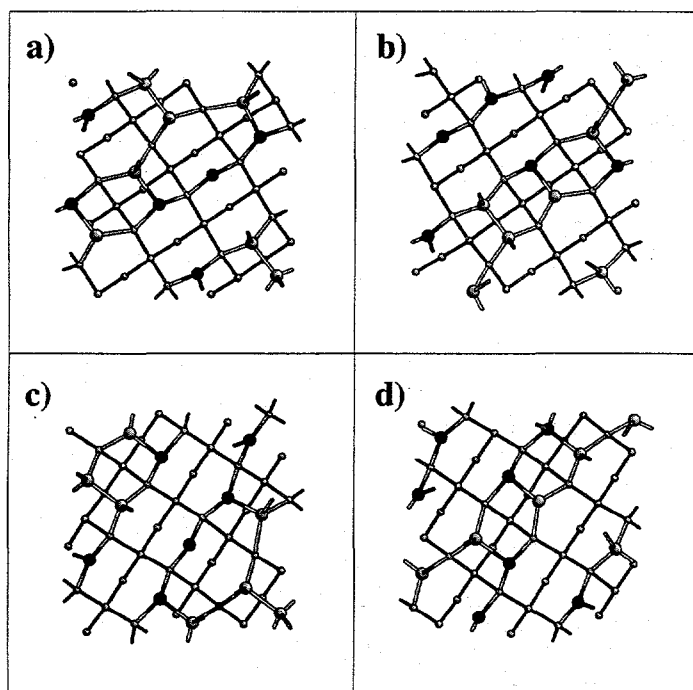

Figure 3. Top view of the individual interface planes for both grain boundaries in the cell. a)-d) are the top and bottom faces of the first and the top and bottom faces of the second grain boundary interface, respectively. Atom appearance is the same as in Fig. 2.

free diamond surface. Many of these bonds are between three-coordinated and four-coordinated atoms, the latter having a bond across the interface. Therefore, these bonds are not double, but they may be stronger than single bonds.

An analysis of bond length distributions in the grain boundary shows that average bond length between two sp^2 atoms is 1.43 Å and the average bond length between sp^2 and sp^3 atoms is 1.51 Å. This suggests that the latter bonds have a partial double bond character since a single bond has a length of 1.54 Å. It was found previously by Cleri for the case of the $\Sigma29$ twist grain boundary that π-bonds across the grain boundary are distorted by a dihedral torsion around the interfacial C-C bond arising from the twist angle of the grain boundary[6]. This distortion is even higher in the case of $\Sigma13$ which has a higher twist angle compared to $\Sigma29$ (67.4° vs 43.6°). Indeed, the C-sp^2-sp^2-C dihedral angle distribution has a peak around 70°. Higher twist weakens the π-bonds across the interface and leads to a higher number of the in-plane dimers, i.e. bonds between carbon atoms belonging to the same interface plane. Some of these dimers are expected to form even for a low twist angle. It was shown in our previous study of the π-bonded stacking fault[5] that if all atoms in the interface are connected by double bonds, we have a high

repulsion between neighboring dimers across the interface due to geometry restrictions imposed by diamond lattice spacings. Formation of some in-plane dimers can lead to a more energetically favorable geometry. Their number steadily increases with increase in the twist angle since the formation of bonds across the interface becomes less favorable due to a decrease in bond order, but energies of in-plane dimers are not affected by the twist.

The stability of the grain boundary is determined by its work of adhesion and it was shown previously by Keblinski *et al.*[2] that (100) grain boundaries have the highest work of adhesion compared to other diamond grain boundaries. We have calculated the formation energy of a $\Sigma 13$ twist grain boundary to be 1.57 eV per interface atom which is about 0.8 eV/atom higher than the energy of a completely double-bonded stacking fault[9]. It also can be compared to 1.25 eV/atom obtained by Wang *et al*[10] using energy minimization with Tersoff potentials. The work of adhesion for the grain boundary is defined as twice the energy of the free reconstructed (100) surface per unit area less grain boundary energy. The calculated work of adhesion for $\Sigma 13$ came out to be 3.52 J/m^2 that is significantly lower than previous molecular dynamics results of 6.2 J/m^2 for $\Sigma 29$.[2] It is expected to be lower because of the higher twist angle and lower number of double bonds across the grain boundary. Part of it can also be attributed to the difference in the methods used in the current and previous studies.

The total density of electronic states and the local density of states for the grain boundary atoms are given in Fig. 4. Both the valence and conduction bands are broadened
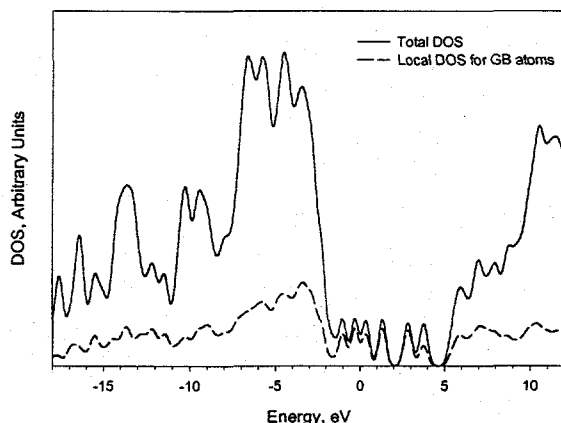

Figure 4. Total and local density of states for $\Sigma 13$ twist diamond grain boundary.

due to the distortion of the tetrahedral bonds in the first two grain boundary layers compared to the bulk diamond and new electron states are introduced at the Fermi level and in the gap. The forbidden gap calculated by the same method for bulk diamond is 6.87 eV. As can clearly be seen from Fig. 4, states in the band gap originate exclusively from the interface atoms.

CONCLUSIONS

In this paper we report on density-functional based tight-binding molecular dynamics calculations of the structure of a twist (100) grain boundary in diamond. About 46% of the carbons in the grain boundary are found to be threefold-coordinated. In addition to bonds across the interface, carbon dimers are formed in the (100) planes in the interface similar to surface dimers on a free diamond (100) surface. Their fraction is proposed to increase for higher twist angle of the grain boundaries. The work of adhesion for $\Sigma 13$

twist grain boundary is calculated to be 3.5 J/m^2. The electronic structure is characterized by a smaller band gap compared to bulk diamond and the presence of electronic levels at the Fermi level and above that are localized on the grain boundary atoms.

ACKNOWLEDGMENT

REFERENCES

1. C. Zuiker, A. K. Krauss, D. M. Gruen, X. Pan, J. C. Li, R. Csencsits, A. Erdemir, C. Bindal, and G. Fenske, *Thin Solid Films,* **270**, 154 (1995).

2. P. Keblinski, D. Wolf, S. R. Phillpot, and H. Gleiter, *J. Mater. Res.,* **13**, 2077 (1998).

3. D. A. Horner, L. A. Curtiss, and D. M Gruen, *Chem. Phys. Lett.,* **223**, 243 (1996).

4. P. C. Redfern, D. A. Horner, L. A. Curtiss, D. M. Gruen, *J. Phys. Chem.,* **100**, 11654 (1996).

5. D. M. Gruen, P. C. Redfern, D. A. Horner, P. Zapol, and L. A. Curtiss, *J. Phys. Chem.,* **103**, 5459 (1999).

6. F. Cleri, P. Keblinski, L. Colombo, D. Wolf, S. R. Phillpot, *Europhys. Lett.,* **46**, 671 (1999).

7. D. Porezag, Th. Frauenheim, Th. Kohler, G. Seifert, and R. Kaschner, *Phys. Rev. B,* **51**, 12947 (1995).

8. M. Elstner, D. Porezag, G. Jungnickel, J. Elsner, M. Haugk, Th. Frauenheim, S. Suhai, G. Seifert, *Phys. Rev. B,* **58**, 7260 (1998).

9. P. Zapol, L.A. Curtiss, D. M. Gruen, *Mater. Res. Soc. Symp. Proc.,* **538**, 371 (1999).

10. Z. Q. Wang, S. A. Dregia, D. Stroud, *Phys. Rev. B,* **49**, 8206 (1994).